UNIL | Université de Lausanne
Faculté de biologie
et de médecine

Hôpital ophtalmique
Jules-Gonin
Service universitaire d'ophtalmologie
Fondation Asile des aveugles

Mémoire de Maîtrise en médecine
N°5806

Evaluation of microRNA mmu-miR-31 influence in degenerative retinal models

Etudiant
Renaud Alexis

Tuteur
Prof. Arsenijevic Yvan
Head of the Unit of Retinal Degeneration and Regeneration
Department of Ophtalmology, UNIL

Co-tuteur
M'Befo Martial, PhD
Unit of Retinal Degeneration and Regeneration, UNIL

Expert
Prof. Schneider Bernard
Neurodegenerative Studies Laboratory, EPFL

Lausanne, 2019

Table des matières

Abstract

Retinitis pigmentosa (RP) is a group of inherited dystrophic retinal disease that affects 1 of 4000 people worldwide. It gradually leads to visual loss through retinal neurodegeneration with a slow and progressive process. The underlying mechanisms of the cell death are now well studied but their interactions remain uncertain. Just before the death of the photoreceptor, some of the cell cycle proteins are reactivated and may play an important role. In the laboratory, some microRNAs have been identified during the photoreceptor relapse of the *Rd1* mouse model of retinal degeneration. The objectives of this study is to understand the potential role of the miR-31 in the control of specific cell cycle proteins. For this experiment, a mouse photoreceptor-like cell line (661W) has been cultured and transfected with a plasmid coding for miR-31 and GFP or a scramble sequence and GFP (control). Western Blot and qPCR allowed us to evaluate respectively the cell cycle protein status and the corresponding mRNA status in relation to the miR-31 overexpression.
Our experiment revealed that miR-31 downregulates E2f1 cell cycle protein in 661W cells. These results must be confirmed with supplementary experiments *in vivo* studies in *Rd1* mouse retina.

Keywords: miR-31, neurodegeneration, retinitis pigmentosa, cell cycle proteins

Introduction

1. The retina

The retina is the nervous layer of the eye. Its role is to detect the visual world and send it to the brain in order to create the visual perception.
The retina is arranged in different layers of cells. The most important one – the outer nuclear layer- is composed from the photoreceptors: the rods and the cones, which are light-sensitive cells and convert the photons energy into an electrical signal and send it via interneurons and the optic nerve to the brain for visual processing. The adult human retina contains more than 5 million cones and about 120 million rods (1). Rod function is to detect dim light in an achromatic vision, while cones are important for the fine visual acuity and for perceiving colours during the day.
Thus said, if the retina is damaged, permanent vision loss or blindness can occur. Age-related macular degeneration, diabetic retinopathy or retinitis pigmentosa (RP) are the most common retinal diseases. The RP is going to be our subject of interest.

2. Retinitis pigmentosa

Introduction, epidemiology and inheritance patterns

Retinitis pigmentosa is composed of inherited dystrophic retinal diseases, which are characterized by progressive degeneration and dysfunction of the retina. The terminology "retinitis" is not accurate, since it is not an inflammatory disease. Other terms like "rod-cone dystrophy", "inherited retinal dystrophy" or "pigmentary retinopathy" may be used.
It affects 1 of 4000 individuals (2) so more than 1,5 million individuals worldwide. It is an early onset disease which usually begins between 5 and 30 years old.
It may be inherited as a dominant, recessive, or X-linked trait or can occur as a sporadically mutation (3). Most of the time this disorder is isolated but also can be part of a syndrome (about 20 – 30% of the cases). There are more than 30 RP-associated syndromes (4). The Usher's syndrome (associated with hearing loss and ataxia) (5) and the Bardet-Biedl syndrome (associated with obesity, cognitive impairment, polydactyly and renal disease) are the two most frequent. More than 100 mutated genes have been related to retinitis pigmentosa (*https://www.omim.org*), but their underlying mechanisms remain for the most unknown.

Clinical manifestations

RP has very heterogeneous manifestations of symptoms, it first can occur during childhood, whereas some other patients will remain asymptomatic until mid-adulthood. One of the earliest symptoms is night blindness, also known as nyctalopia. Due to constant presence of artificial light during night time, this symptom may be never noticed by some patients and the identification of the disease can be delayed. Another common feature is the progressive constriction of the visual fields. First, the patient will notice a loss of the mid-peripheral visual field, which will evolve to the loss of far-peripheral vision. Then, they will develop tunnel vision and eventually lose their central vision about age 30 or much earlier depending

on the mutation. A typical, but late-onset manifestation of the RP, is a decreasing visual acuity, due to loss of the cones, leading finally to blindness.

Diagnostics, treatments and prognosis

The diagnostic of retinitis pigmentosa can be done with the combination of the patient's history and some complementary examination. One of the most important assessment is done with the fundus exam, on which we can see pigmentary changes, as dark spots in the periphery of the retina, and pallor on the optic nerve. A patient with RP will have a constrictive visual-fields measured by the Goldman perimetry and the ERG (electro-retinogram; which measures the electrical response of the retina to light stimuli) will show reduced response amplitudes and a delay in their timing (6).
No approved treatment currently exists (7) and this disease often leads to blindness. Actually, research is focused on the slow-down of the evolution of the disease with strategies like gene therapy, cell transplantation and some treatment like retinal prosthesis are actually tested (8).

3. Retinal neurodegeneration

The mechanisms at the origin of the photoreceptor's death in the RP are now well studied. Initially, it was thought that retinal photoreceptor's death was due to mechanism like apoptosis (9). However, neurodegeneration in photoreceptor seems to be a much slower mechanism than apoptosis and does not involve the main actors inducing apoptosis (10). Distinct pathways are implied. In fact, studies show that the underlying mechanism of retinal degeneration is more complex.
Retina from a mouse model with deficient gene for the ß subunit of phosphodiesterase (PDE6ß), *Rd1* mice, are habitually used for the investigation on retinal degeneration (11). Many cellular pathways were observed to be activated or altered during the photoreceptor degeneration process. For instance, it was seen that cGMP (Cyclic guanosine monophosphate) and PKG (Protein kinase G); which are two well-known regulators of intra-cellular activity, had an increased level in these *Rd1* mice, and that their inhibition *in vitro* could lead to moderate cell rescue (12). Other processes like calpain-type protease activation (13), increased calcium (14) and oxidative stress (15) are also fairly suspected. Moreover, an increased PARP (-*protein involved in the DNA repair*) level was also identified in *Rd1* mice (16) and was therefore a well-studied protein for the retinal degeneration. Therefore, an alternative molecular pathway to cell death degeneration involving CREB (-*transcription factor*) downregulation, oxidative stress, PARP overactivation and cyclic nucleotide deregulation was proposed (17), but the attempts to protect the photoreceptors cells from death in *Rd1* retina by acting on these pathways are not fully satisfying. A more recent study, which alternatively investigated the cell cycle proteins in *Rd1* retina, found that these proteins were increased in photoreceptor before death (18) and that a reduced level of BMI1 (polycomb group protein regulating proliferation) could lead to a significant cell rescue. Indeed, some cell cycle protein may have a second role in certain post-mitotic cells (19). The cell cycle is therefore reactivated before the death of the photoreceptors (20). Analogous results were found for neurological degenerative diseases as Alzheimer (21) and Parkinson disease (22) which comforts us in the idea that retinal degeneration is very similar to neurodegeneration in the whole nervous system. The inhibition of the re-entry in the cell

cycle in *Rd1* retina appears to cause a massive cell protection (17, 22) and this could consequently lead to potential new pharmacological treatment. This all brought us to focus our study on the cell cycle protein, as we suspect them to have a major role in the retinal neurodegeneration.

4. MicroRNA-31

MicroRNA (miR) are small non-coding RNA, ranging from 21 to 25 nucleotides in lenght. They are a major class of regulatory molecule in animals and plants (24). They can control the genetic expression at a post-transcriptional level by binding the 3'-untranslated region (3'UTR) of the messenger RNA (mRNA), and induce an inhibition of the expression.
MiRs are more and more studied as we slowly discover considerable role in development, homeostasis, differentiation and especially proliferation. Depending on the context, miR can promote cancer cell proliferation (25) as an oncogene; or on the contrary, be a tumor suppressor as in the gastric cancer (26) or in the ovarian carcinoma (27). Their association with the cell cycle is admitted (28) and we know them to be involved in retinal diseases since they have been identified as modulating diabetic retinopathy (29).
The role of the miR-31 has been studied and results showed that it promotes angiogenesis (30), cancer cell proliferation in colorectal carcinoma (31) and is reduced in ischemic retinas (32). MiR-31 also have opposite functions depending on the tumoral context (33). Furthermore, a cell cycle protein, E2f2, has been identified as being a target of miR-31 (34), which brought us to assume that, among other miRs, miR-31 was a main regulator of cell-cycle protein. By comparing *Rd1* retina with *wt* (wild type) retina, our lab recently evidenced a considerable decreased amount of miR-31 in the retinal degeneration and therefore, this reduced quantity is suspected to be associated with the cell cycle protein activity. Our hypothesis was that an increased miR-31 concentration in *Rd1* retina will block the cell cycle re-entry and thus slow down the cell death process.

Aims of the study

The objective of our experiment is to understand the effect of a miR-31 overexpression on retinal cell proliferation and cell cycle protein. For that, we decided to transfect a plasmid expressing miR-31 in 661W photoreceptor-like cells and evaluate through Western-Blot and RT-qPCR the effect it can have on proteins and genes regulating the cell cycle such as E2F1, CDK4, E2f4, FoxM1 and Chk1. Based on what was previously introduced, we expected a decreased amount of these targets.

Materials and methods

1. Plasmid and cell line

A miR-31 plasmid, which was composed of pEZX-MR04 vector with an antibiotic resistant gene, a GFP-expressing gene and a CMV promoter, was used during the experiment. As well as a GFP-expressing plasmid.
The cell line tested on this study was the 661W cell line.

2. Plasmid amplification

One of the first steps was to amplify our DNA plasmids expressing the miR-31 coding sequence and GFP control into a lot bigger amount in the process called transformation.
For bacterial transformation, we used the DH5 alpha electro competent cells. 1 µL of each plasmid was incubated with 50 µL aliquot of DH5 alpha, well mixed with gentle agitation before electroporation (with BioRad Micropulser™). After 1 h incubation of the mixture in minimal medium (S.O.C), 20 µL of the cell solution were plated on LB agar with ampicillin antibiotics for selection of successful transformants. For homogeneous distribution of the cell suspension on the LB agar plate, we added autoclaved glass beads (4 mm diameter) and did a gently shake to spread the cells. The plate was then incubated at 37°C overnight to allowed colonies to form.

3. Bacterial growth and prepping

The next day, we used a pipette tips to carefully pinch a single colony and transfer it into tube containing a mix of 2 mL of LB medium and 2 µL of ampicillin. The mix was then incubated at 37°C incubator, 300 rpm for more than 6 hours. 1 mL of the mini culture was used for large scale DNA amplification in 500 mL Erlenmeyer containing 200 mL of LB medium and 200 µL of ampicillin overnight at 37°C, 300 rpm.

4. DNA purification

This bacterial proliferation possesses a great number of DNA which express the miR-31 gene. The next objective was to isolate and collect the DNA. To this end, we used a commercial kit, NucleoBond® maxi, and carefully followed the manufacturer's instructions. After the cell lysis with several buffers, DNA was bind to the column filters and was collected in a new ent through the gravity. DNA precipitation was performed with room temperature isopropanol, followed by a centrifugation at 15'000 g for 45 minutes at 4°C. Then, ethanol 70% allowed the solution to be correctly washed, before being extracted after the centrifugation at 15'000 g for 5 minutes at 4°C. Purified DNA was reconstituted in 50 µL of sterile HBSS and 1 µL was assayed on -NanoDrop®- to assess the DNA concentration and purity.

5. 661W cell culture and growth assay

The 661W cells were cultured in Dulbecco's modified Eagle's medium (DMEM), 10% fetal bovine serum (FBS), 1% penicillin/streptomycin (P/S) antibiotic and 0,5 mM of ß-mercapto-ethanol, in humidified incubator at 37°C, and 5% CO2. The cells were maintained in culture flasks, usually 150 mm^2 or 75 mm^2 until 80% to 90% of confluence, and media were refreshed every 4 days. Our passaging process was as follow: the medium was aspirated; adherent cells were washed with 5 mL of Hank's balanced salt solution (HBSS) during a few seconds, then detached with 0,5 mL of Trypsin, during 3 minutes at 37°C and peeling of was inhibited with complete media. Cells were pelleted by centrifugation for 3 minutes at 800 turn per minute and then re-suspended in 5 mL of DMEM medium. We then took the necessary proportion of volume, according to the desired passaging, to seed in a new flask. Finally, we checked the flasks at the microscope to ensure that the suspended cells were well separated and free of aggregates, before incubating the flasks at 37°C.

6. Transfection of 661W cells with vector expressing micro-RNA

Transient transfection is the introduction of purified DNA into a cell. It can be performed through different techniques such as electroporation, calcium phosphate or lipofection. We used this last technique for our transfection: a cationic lipid was mixed with the DNA to form liposome, this complex will then fuse with the membrane of the target cell, and drop the DNA material inside.
About 12 to 24 hours before the transfection, 1.2x 10^5 and 6x10^4 cells were seeded on 12-well plates (in 2 mL of growth medium) or 24-well plates (1 mL of growth medium) respectively, so that the confluence will be about 70-80% during the transfection.
The transfection was performed in triplicate for each plasmid, using the HBSS buffer as control. Cells were transfected with lipofectamine® 2000 transfection reagents and lipofectamine® 3000 transfection reagents according to the manufacturer protocol. Briefly, the actual cell medium in the well plate was aspirated and replaced with OPTI-MEM which is a reduced serum media. The following process is described for one 12-well, and was repeated for the necessary number of wells. In a first tube, lipofectamine reagent 2 µL was diluted in OPTI-MEM 50 µL and well mixed by 2-3 seconds of vortex. In another tube, 1 µg of DNA was diluted in 50 µL of OPTI-MEM, and 2 µL of P3000 reagents was added. The diluted DNA (and P3000 reagents) was added drop by drop in the lipofectamine tube, which was incubated during 5 – 10 minutes at room temperature. After the DNA-lipid complex was well formed, 100 µL of this mix was gently distributed in the corresponding well and then incubated at 37°C so that the DNA complex could be fully integrated and expressed in the 661W cells. The media was replaced 6 h post-transfection and the plates were incubated back in the incubator for 48 h to allow transgene expression.

7. Generation of total cell homogenate

The cells were harvested by scraping, and transferred into a 1.5 mL micro centrifuge Eppendorf tube. Then pelleted at 300 g, 4°C during 10 minutes. Cells were washed in phosphate buffer saline (PBS) 500 µL, pelleted as above, and lysed in 150 µL of Radioimmunoprecipitation assay (RIPA) Lysis Buffer (10 mM Tris [pH 8], 1 mM EDTA, 140 mM NaCl, 1% Triton, 0,1% SDS, 0,1% Na-deoxycholate) with cell lysis supplements (1%

proteases inhibitors cocktails, 1% phosphatases inhibitors, 1 mM phenylmethylsulfonyl fluoride (pmsf)). The cells were lysed up and down with pipette and then incubated on ice for 30 minutes with constant vortexing each 5 to 7 minutes. The cell debris was then pelleted by centrifugation 16'000 g, at 4°C during 10 minutes. The supernatant, which contains the whole cell lysate, were finally collected into a clean Eppendorf tube and immediately stored at -80°C until the day of analysis.

8. BCA assay

Bicinchoninic acid assay (BCA assay) is a colorimetric technique that measure the total concentration of protein in a solution. Our BCA assay was done in a 96-well transparent plate. First, we prepared the standard solution, with a serial dilution from the stock solution at 2 µg/µL bovine serum albumin (BSA) diluted in our RIPA lysis buffer, so that the BSA concentration was known, in a final volume of 50 µL. Next, the sample dilution was performed, with 5 µL of sample diluted in 45 µL of RIPA lysis buffer. All the solutions were then well mixed up and divided in two, by pipetting 25 µL of each well side down to a clear well, for a final volume of 25 µL. BCA reagents mix of 200 µL were added in each well, followed by a gently shaking during 30 seconds at room temperature, and then incubated during 30 minutes at 37°C. Finally, the absorbance was read on MRX II microplate absorbance reader (Dynex Technologies) at a wavelength of 562 nm.

9. Western blot analysis

Western blot is a biomoecular technique that allows the detection and identification of proteins in a certain solution. It uses antibodies: the primary antibody, which is specific for a protein of interest, and the secondary antibody, which binds the first one and permits the detection and visualization through chemiluminescence, fluorescence or other detection techniques.
Based on the BCA assays, the total protein of the samples sets was normalized to the same concentration. The samples were mixed with protein loading buffer (5x) and boiled at 95°C during 5 min for denaturation.
15 µL of protein sample (and 2,5 µL of protein marker) were resolved on 10% Polyacrylamide gel electrophoresis (Acryl 5 mL, 1,5M Tris [pH 8.8] 5 mL, 20% SDS, H2O 9,8 mL, 10% APS 200 µL, Temed 8 µL) at constant 140 V for 70 minutes. This process allows the protein with an electrical charge to migrate through the gel, according to their molecular weight.
Proteins were transferred into a nitrocellulose membrane during 90 minutes at 500 mA, immersed in a transfer buffer (for 1 L: Ethanol 20%, 0,58 g Tris (48 mM), 0,29 g Glycin (39 mM), SDS 10%). For this, the membrane was placed next to the gel, sandwiched between blotting paper and sponges and clamped tightly between solid brackets. The nitrocellulose membrane was stained with Ponceau Red to check for the quality of the transfer, then washed thoroughly with water, tris-buffered saline (TBS; for 500 mL: Tris 12.1 g, NaCl 87,7 g, H20 up to 500 mL) and TBST (TBS + 0.1% Tween 20) until the membrane was completely de-stained.
To prevent non-specific interactions, it was further incubated 1 h with odyssey blocking buffer (PBS 3:1 TBS) at room temperature to prevent non-specific interactions. The membranes were incubated ON with the primary antibody solution prepared in odyssey blocking buffer with 0.1% tween 20 as indicated in *table 1*.

The next day, the membrane was washed 3 times with TBST, 5 min per wash with shaking to remove unbound antibodies.
AlexaFluor ® 488 or 633 conjugated secondary antibody was used for a 1-hour incubation at room temperature, with gently shaking and protected from light.
The membrane was then washed 2 times with TBST and once with PBS, 5 min per wash and put under infrared light for the detection and identification of the protein bands, which will next be interpreted and analyzed by densitometry.

Name	*Origin*	*Fabrication*	*Dilution*
Primary antibodies (IgG)			
E2F1	rabbit	Santa Cruz	1:500
CDK4	rabbit	Santa Cruz	1:500
GFP (G6)	mouse	Santa Cruz	1:2000
Histone (H3)	rabbit	Santa Cruz	1:10000
Secondary antibodies (IgG)			
alexa fluor® 488 anti-mouse	goat	Invitrogen	1:15000
alexa fluor® 488 anti-rabbit	goat	Invitrogen	1:15000
alexa fluor® 633 anti-mouse	goat	Invitrogen	1:15000
alexa fluor® 633 anti-rabbit	goat	Invitrogen	1:15000

Table 1: *List of antibodies used during the experiment;* Alexa fluor® 488 *emitted green light at a wave length of 519 nm, whereas* Alexa fluor® 633 *emitted red light at 647 nm.*

10. Total RNA extraction and precipitation

The total RNA was extracted using RNAzol® reagent (Sigma) according to manufacturer's instructions. Briefly, cells were thaw from -80°C and lyzed in 200 µL RNAzol RT and then put in an Eppendorf tube with 80 µL of RNase-free water during 5-15 min. Centrifugation separated the mixture into a semisolid pellet (containing DNA, proteins and polysaccharides) and an upper supernatant (containing the RNA) that we carefully placed in a new tube with 2.5 volume of isopropanol to precipitate the RNA. After washing with 300 µL of 75% ethanol to the RNA pellet was solubilized in 15 µL RNase-free water on ice to avoid unexpected degradation. The quality of the purified RNA was further assessed by spectrophotometry technique using NanoDrop® technology.

11. RT-PCR

Our objective was to assess the amount of mRNA of specific genes. To that aim we needed first to produce the cDNA corresponding to these mRNAs. Reverse transcription (RT) reaction is a technique that allows the transcription of RNA into cDNA. It is done thanks to an enzyme, the reverse transcriptase, which is mixed with random primers to ensure the initiation of the synthesis of cDNA with mRNA. RT also requires a mix of nucleotides for the DNA synthesis and various RT buffers

The RNA solution was standardized to a 100 ng/µL concentration in 10 µL of RNAse free water. RTs were performed in 20 µL of solution per 200 µL PCR tubes, with 10 µL of 2X RT master mix (see *table 2*). The tubes were loaded on the thermal cycler which allows the RT reactions to happened according to a 4-steps cycle program as seen on *table 3*. To avoid RNase contamination, all these steps were performed with RNase-free consumables and in a RNase-free environment.

Component	*Volume per reaction*
10X RT buffer	2.0 µL
25X dNTP mix (100mM)	0.8 µL
10X RT random primers	2.0 µL
MultiScribe™ Reverse Transcriptase	1.0 µL
RNase inhibitor	1.0 µL
Nuclease-free H20	3.2 µL
Total per reaction	*10.0 µL*

Table 2: *2X RT master mix receipt. The volumes presented on this table are for one unique reaction. The master mix was prepared after calculation for the required number of reactions.*

	step 1	step 2	step 3	step 4
temperature (C°)	25°C	37°C	85°C	4°C
time (minutes)	10	120	5	undefined

Table 3: *Thermal cycling program for reverse transcriptase reactions.*

12. QPCR analysis

Real-time Polymerase Chain Reaction (real-time PCR) or quantitative PCR (qPCR) is a technique of biology based on the amplification of DNA or cDNA. QPCR monitors in real-time, the amount of a known amplicon in a sample. Since this cDNA comes from a mRNA of a specific gene, it will give us the indirect expression of our gene of interest.
A 96-well reaction plate was loaded with a 2X qPCR SYBR green master mix 10 µL, 2,5 µM primers (2,5 µL forward primers and 2,5 µL reverse primers) for Chk1, E2f4 and FoxM1 (sequence available on *table 4*) were used for the PCR, with 5 µL of cDNA sample. We performed a serial dilution until a final amount of 0,05 ng of cDNA. Amplifications were done according to the manufacturer's protocol using the LightCycler ® 96 (Roche) which also allows to analyse the standard and melting curves and the average Ct of each reactions.

Gene	*Sequence*
Chk1 (forward)	5'-CTGGAGTACTGTAGTGGAGGAG-3'
Chk1 (reverse)	5'-CCGAAATACCGTTGCCAAGCC-3'
E2f4 (forward)	5'-CTCAATGGCCAGAAGAAGTACC-3'
E2f4 (reverse)	5'-CTCACTGCAATCTCAGATGTCG-3'
FoxM1 (forward)	5'-GCTTGCGATTCTCGATGGAGAG-3'
FoxM1 (reverse)	5'-CTGGACACTGCCACCTCTTG-3'

Table 4: *Sequence of the forward and reverse primers used during the experiment.*

Results

- Set up of 661W cell culture conditions to obtain optimal conditions for miRNA transfection

To better understand the molecular basis of eye diseases and facilitate the investigations, cell lines are usually used. The 661W cell, is a well-known mouse photoreceptor-like cell line (35). It is derived from a retinal tumor and express several markers of cone photoreceptors. Because these cells are proliferating and because the miRNA we aim to test may affect cell proliferation, we hypothesized that this cell line may be appropriate. To perform an efficient miRNA transfection on the 661W cells, we wanted to have optimal conditions. This is why we decided to observe and understand their growth kinetic in 12-well plate and 24-well plate.

Various amounts of 661W cells were put on culture and we evaluated the confluence of the cells after a certain amount of time. For each well, we wanted to know which amount of cell was required for having a 70-80% confluence the next day. This amount of confluence was recommended by the manufacturer for an efficient lipofectamine® transfection of our plasmid expressing miR-31.

For the 12-well, we put on culture 80'000, 120'000, 160'000 and 200'000 cells per mL, and for the 24-well plate 40'000, 60'000, 80'000 and 100'000 cells per mL, then observed their density and confluence after 24 hours, 48 hours and 72 hours. The results are presented on *figure 1*. We observed a linear correlation between the number of cell seeded and the time required to achieve confluence.

The cell confluences were subjectively measured with microscope. In the two plates, 200'000 cells/mL corresponded to about 60% to 70% of confluence, 400'000 cells/mL were about 80% and 600'000 cells/mL and more, exceeded the 95% of confluence.

For the 12-well plate, we observed that 80'000 cells seeded, allowed to reach about 50-60% of confluence after 24 hours and almost 80% after 48 hours, whereas 120'000 cells seeded reached the confluence of 60-70% at 24 hours.

In a parallel way, we observed for the 24-well plate, a bit more than 70% of confluence for the 40'000 density after 48 hours. The wells with 60'000 cells per mL reached almost 60-70% confluence at 24 hours and over 80% after 48 hours. These two values were not so dissimilar, but we decided to stick to the 60'000 cells per mL. Indeed, all the following density of cells tested for the 12-well plate and the 24-well plate (160'000, 200'000 cells/mL and 80'000 and 100'000 cells/mL respectively) were rapidly too confluent and reached more than 95% of confluence too briefly so that we were not comfortable with our study.

Therefore, we concluded that 120'000 cells seeded per mL on the 12-well plate and 60'000 cells per mL for the 24-well plate were the optimal amount of 661W cells to achieve the cellular density we needed for the miR-31 transfection protocol.

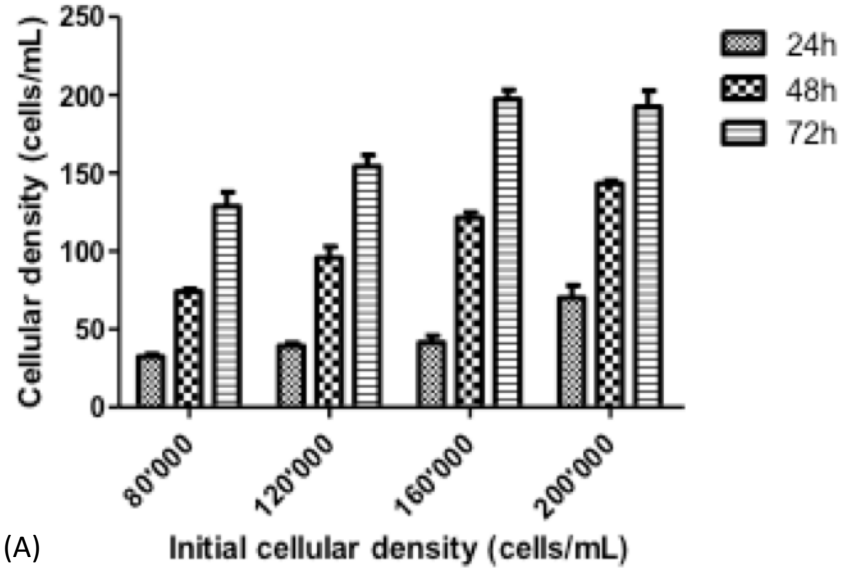

(A)

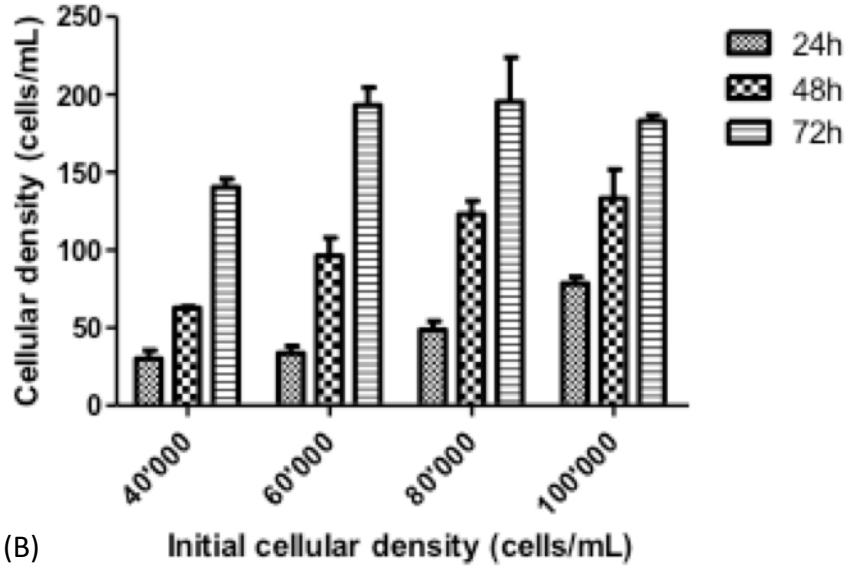

(B)

Figure 1: *Time course of 661W cell density in function of cell number seeded initially; (A) is the 12-well plate study and (B) is the 24-well plate study. The errors bars indicate the SEM. The cellular density increased proportionally to time and number of cells seeded.*

- Effective 661W cell transfection with GFP and miR-31 cDNA: fluorescent detection on microscope

As we wanted to evaluate the effect of the miR-31 overexpression on the 661W cell proliferation, we performed a transfection with a plasmid expressing the miR-31 gene as well as the Green Fluorescent Protein (GFP) gene and let the cells express these genes for at least 48 hours. With the reporter gene, we can detect the expression of the transfected plasmid on microscope, and therefore, validate the transfection in the cells.
The lipofectamine transfection experiments were performed under three conditions, first with the HBSS only for the negative control, the second with a plasmid coding only for GFP as the positive control and the last with the miR-31 plasmid. The transfected cells were then analysed with a fluorescent light microscope, as seen on the microscope images presented on *figure 2*. We estimated a transfection efficiency below 20% and 10% for the miR-31 plasmid and for the control plasmid, respectively.

- WB analyse of the 661W cells transfected with miR-31

Cell lysate was generated 48 hours after the transfection. Therefore, the transfected cells had this time lapse to overexpress the miR-31 and undergo the molecular changes that we expected to identify. We harvested the whole cell population in the 12-well, the cells that received an efficient transfection and the ones that did not.
The total protein concentration for each sample was measured with BCA assays as explained in *materials and methods* section and then diluted on the same concentration for the Western Blot. The red ponceau staining revealed that the WB transfer on the membrane was successful (*figure 3*). We observed that some samples contain more protein, for example in GFP-1, GFP-2, miR-31-1, miR-31-2, miR-31-3 and miR-31-4. This variability may be due to any previous step in the manipulation (protein preparation, gel loading etc.) or to the treatment and must be taken into account for the interpretation of the results.

- Test of the expression of the vectors

GFP sequence was present in both plasmids and served to validate the efficiency of the transfection. The GFP protein is known to have a molecular weight of 27 kDa, which corresponds precisely where the band is revealed on *figure 4*. We can therefore conclude that there is no GFP protein in the HBSS-1, HBSS-2, HBSS-3 and HBSS-4 samples which correspond to the negative control. As expected, in the GFP-1, GFP-2, GFP-3, GFP-4, miR-31-1, miR-31-2, miR-31-3, miR-31-4 samples, GFP protein was well expressed.

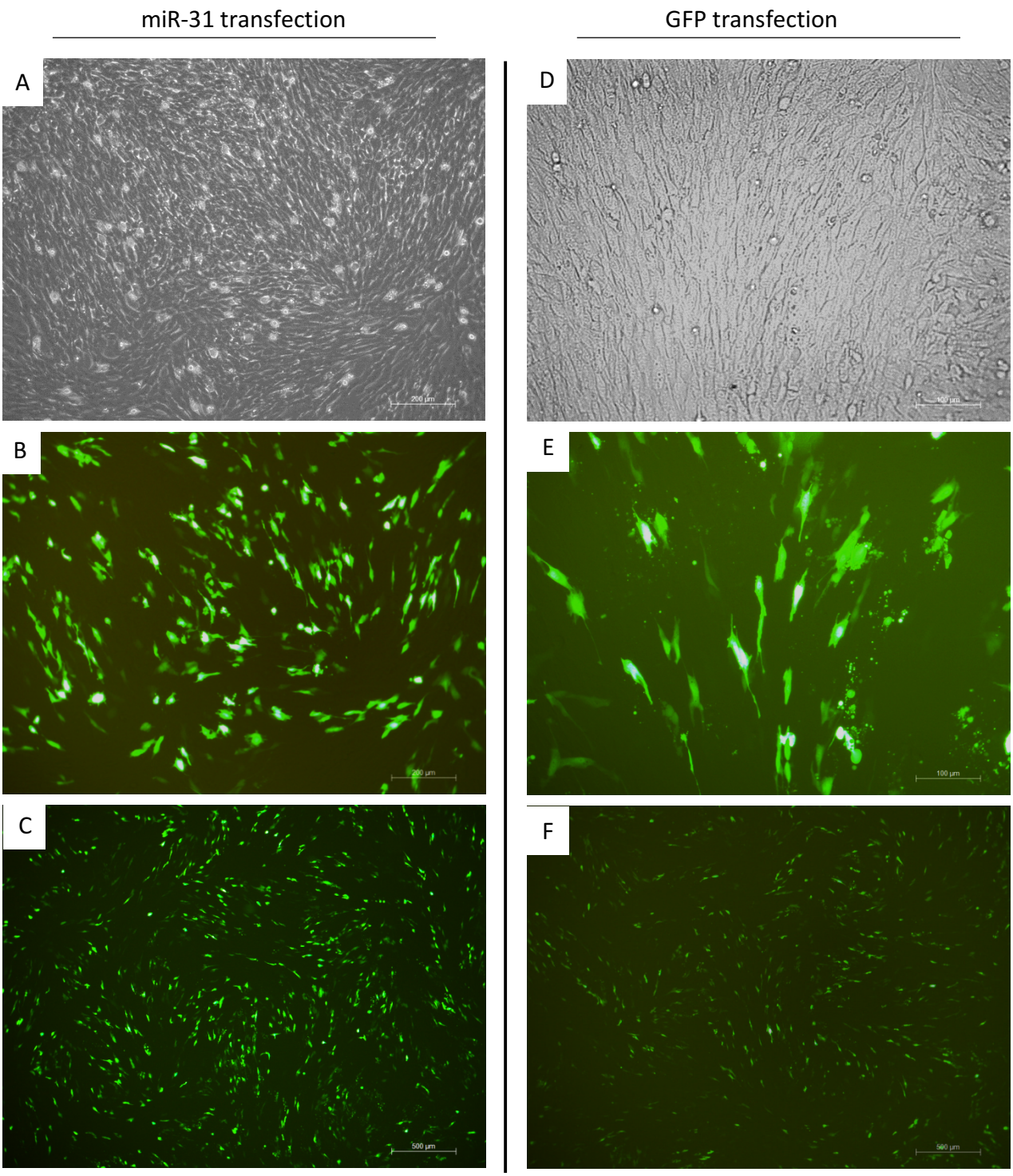

Figure 2: *Transfection of 661W cells. (A, D) Phase contrast picture of cells after transfection (Black and white. (B, C) Green fluorescent protein (GFP) expression 48 h after miR-31 transfection of 661W cells. (E, F) GFP expression after GFP-scramble control transfection of 661W cells. We estimate a transfection efficiency of <20% for the miR-31 construct and <10% for the control plasmid. Scale bars are shown in each panel.*

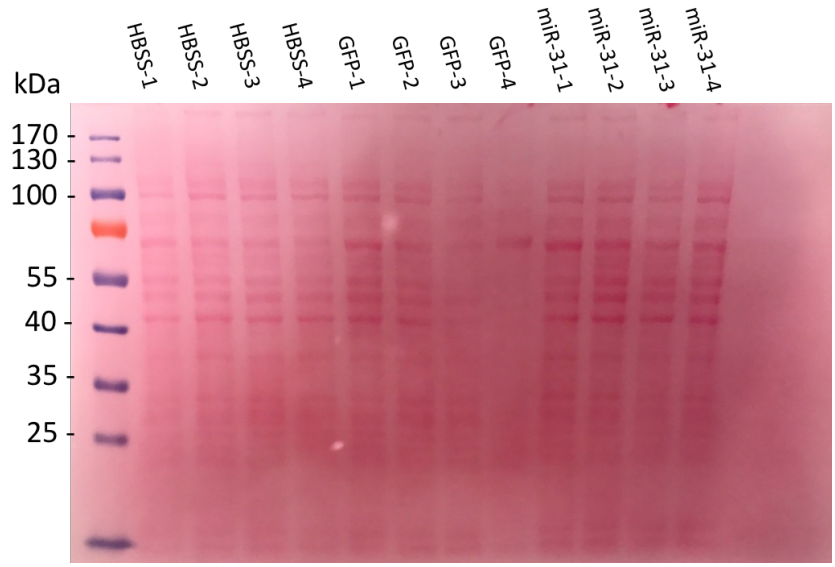

***Figure 3**: Protein transfer evidenced by Red ponceau staining. The left lane is the protein marker used as ladder according to the molecular weight (in kDa) as indicated.*

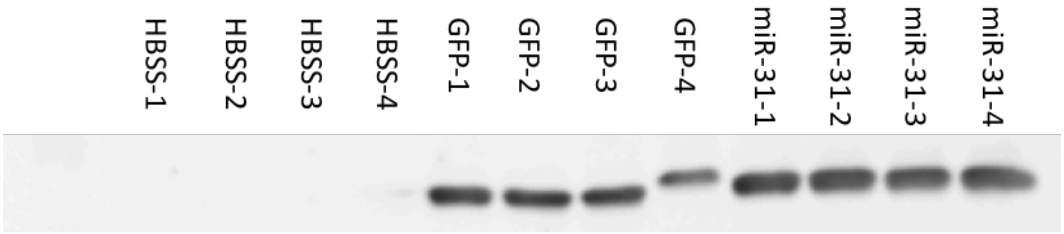

Figure 4: *WB analysis of a membrane incubated with GFP protein antibodies. Protein band corresponding to 27 kDa molecular weight are visualized in the GFP-1, GFP-2, GFP-3, GFP-4, miR-31-1, miR-31-2, miR-31-3, miR-31-4 samples, but not present in the HBSS-1, HBSS-2, HBSS-3 and HBSS-4 samples.*

- Reduced E2F1 in miR-31 transfected 661W cells

The listed antibodies on *table 1* were applied to the membrane as explained in *materials and methods.*
Anti-E2F1 and anti-CDK4 antibodies were used with the anti-Histone H3 antibody in order to have a protein level as a normalizing control. E2F1 and CDK4 were the protein of interest as they are cell cycle proteins, and we expected their level to decrease in the experimental condition, compared to the control condition.
Figure 5 shows the WB analysis, the first membrane *(A)* was incubated with E2F1 and H3 antibody solution and the second membrane *(B)* with CDK4 and H3 antibodies. The molecular weight corresponding to the migration of the protein visualized on the

membranes indicates us that the proteins E2F1 (61 kDa), Histone H3 (18 kDa) and CDK4 (34 kDa) are detected on the WB.
Then, we compared and analysed with densitometry the intensity of the bands, which correspond to the protein concentration. Then, the values for E2F1 and CDK4 bands were normalized with each corresponding H3 protein signal. For each quadruplicate, we calculated the average, the standard error of the mean (SEM) and *p* values (levels of significance: $p < 0.01$ is considered as highly significant (**), $p < 0.05$ as significant (*) and $p > 0.05$ as non-significant (ns)).

The densitometry (*figure 6*) showed that the amount of E2F1 protein was significantly reduced in the miR-31 sample compared to the non-treated (NT) sample and the GFP-treated sample (GFP treated: 1.614 ± 0.166 SEM, n = 4; miR-31 treated: 0.444 ± 0.108, n = 4; p = 0.001). Regarding the CDK4 densitometry, we observed a slight, but unsignificant difference between the GFP-treated and the miR-31 treated samples. In conclusion, this result revealed that a 48 hours miR-31 overexpression in 661W cells induce a reduction in E2F1 protein expression.

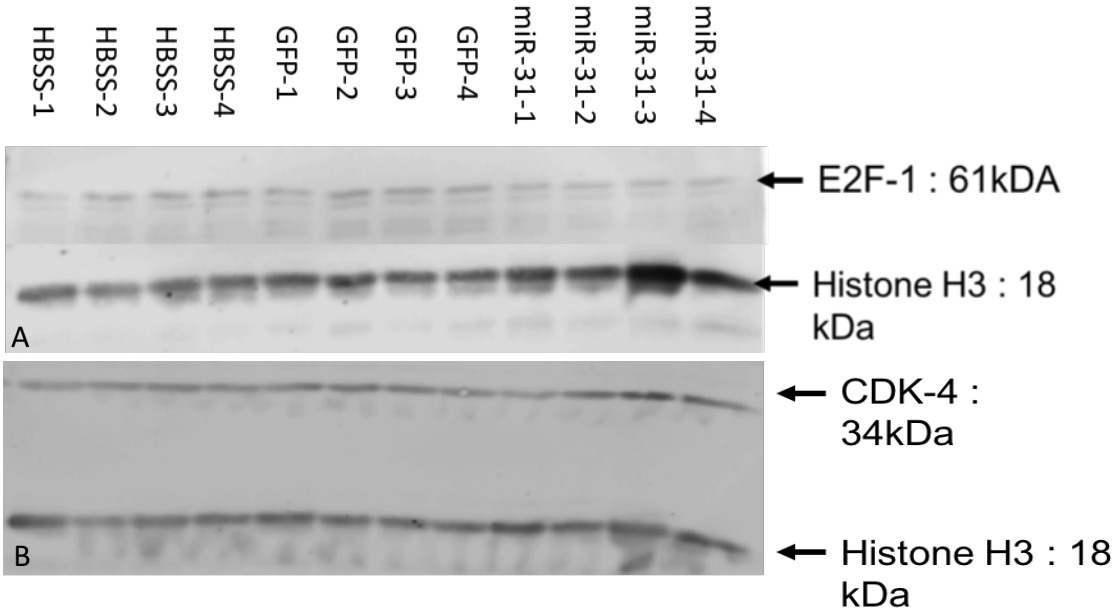

Figure 5: *Effect of miR-31 overexpression on cell-cycle proteins regulating G1 and S-phases. WB analysis of the membrane incubated with antibodies for E2F1 and H3 protein (A) and the membrane incubated with antibodies for CDK4 and H3 protein (B). Note the reduced level of E2F1 after miR-31 transfection.*

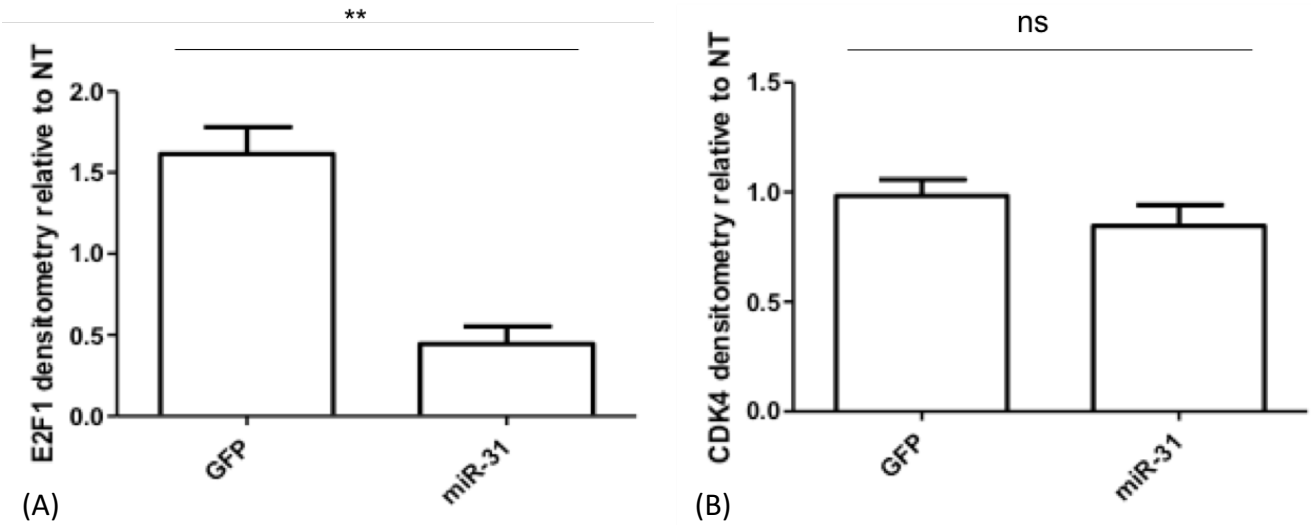

Figure 6: *Effects of miR-31 transfection on cell-cycle proteins in the 661W cell; Expression levels of E2F1 (A) and CDK4 (B) were analyzed by WB 48 h after the transfections of the different constructs. Errors bars indicate the SEM. Note the highly significant reduction of E2F1 in the miR-31 group (p = 0.001). No significant differences were observed between groups for the CDK4 expression.*

- Spectrophotometry: Total RNA concentration in the transfected 661W cell samples

Another way for evaluating the expression of a gene, is to quantify the mRNA amount of the gene of interest. To that purpose, we extracted and isolated the total RNA from the 661W cells, 48 hours after their transfection, according to the protocol previously described.
The extracted pellet was submitted to a Nanodrop® spectrophotometry measurement (*table 5)* and the purity of the sample was considered satisfactory when the 260/280 ratio was over 1.8. Sample #1 is a blank measure and sample #7, #13 and #14 were eliminated because of a too little RNA concentration. The RNA concentration of the samples varies between 717.6 ng/µL (for the 4th GFP sample) and 982.7 ng/µL (for the 3rd GFP sample) and the 260/280 ratio varied between 1.98 (for GFP-4 and miR-31-1 samples) and 2.01 (for the HBSS-1 sample). We normalized the concentration of the following samples: HBSS-1, HBSS-2, HBSS-3, HBSS-4, GFP-1, GFP-3, GFP-4, miR-31-1, miR-31-2 and miR-31-3 and performed the reverse transcription reactions.

#	Sample ID	User name	Date and Time	Nucleic Acid Conc.	Unit	A260	A280	260/280	260/230	Sample Type	Factor
1	DEPC	Nanodrop	28.08.2017 14:15:58	0.1	ng/µl	0.001	-0.014	-0.10	0.00	RNA	40.00
2	HBSS1	Nanodrop	28.08.2017 14:17:40	944.2	ng/µl	23.606	11.767	2.01	2.03	RNA	40.00
3	HBSS2	Nanodrop	28.08.2017 14:18:36	895.6	ng/µl	22.391	11.254	1.99	2.20	RNA	40.00
4	HBSS3	Nanodrop	28.08.2017 14:19:20	933.1	ng/µl	23.328	11.687	2.00	2.12	RNA	40.00
5	HBSS4	Nanodrop	28.08.2017 14:20:07	761.3	ng/µl	19.032	9.508	2.00	1.85	RNA	40.00
6	GFP1	Nanodrop	28.08.2017 14:20:51	823.3	ng/µl	20.583	10.461	1.97	2.13	RNA	40.00
7	GFP2	Nanodrop	28.08.2017 14:21:29	7.7	ng/µl	0.193	0.105	1.83	0.28	RNA	40.00
8	GFP3	Nanodrop	28.08.2017 14:22:12	982.7	ng/µl	24.568	12.364	1.99	2.24	RNA	40.00
9	GFP4	Nanodrop	28.08.2017 14:22:54	717.6	ng/µl	17.939	9.039	1.98	2.23	RNA	40.00
10	mmu-mir-1	Nanodrop	28.08.2017 14:23:45	935.4	ng/µl	23.384	11.813	1.98	2.25	RNA	40.00
11	mmu-mir-2	Nanodrop	28.08.2017 14:24:27	973.8	ng/µl	24.346	12.223	1.99	2.16	RNA	40.00
12	mmu-mir-3	Nanodrop	28.08.2017 14:25:02	858.0	ng/µl	21.449	10.759	1.99	2.21	RNA	40.00
13	mmu-mir-4	Nanodrop	28.08.2017 14:25:40	360.7	ng/µl	9.018	4.838	1.86	1.25	RNA	40.00
14	GFP2.1	Nanodrop	28.08.2017 14:26:48	8.5	ng/µl	0.212	0.120	1.76	0.28	RNA	40.00

Table 5: *Screenshot of Nanodrop® table; with Sample ID, nucleic acid concentration (ng/µL), 260 and 280 wavelength absorbance, 260/280 absorbance ratio. DEPC is diethylpyrocabonate-treated water (blank measurement).*

- Decreased Chk1 and E2f4 gene expressions in miR-31 transfected 661W cell

The qPCR is the technique that allowed us to quantify the mRNA amount of our genes of interest. During 48 hours, the transfected 661W cells produced mRNA under three different conditions. Our hypothesis was that Chk1, E2f4 and FoxM1 genes might be less expressed with a miR-31 overexpression, because they are regulating the cell cycle. So we performed an experiment based on one qPCR amplification of cDNA using forward and reverse primers for Chk1, E2f4, FoxM1 and Mrl8 genes and measured the load of amplicon for each of them in 3 replicates (n = 1).
A comparative Ct method (ΔΔCt method) was used for the data analysis (*table 6)*. The results of the genes of interest (Chk1, E2f4, FoxM1) were normalized with a gene ubiquitously expressed in different cells (Mrl8). The values of the two treated conditions (GFP transfection and miR-31 transfection) were then compared with the NT condition (HBSS). *Figure 7* presents the expression fold changes for each gene in the GFP treated and miR-31 treated samples, relative to the NT.
The expression fold change for Chk1 and E2f4 are lower in the miR-31 condition than in the GFP condition. So, with the miR-31 treatment, we do observe a reduction of expression of Chk1 gene and E2f4 gene. Unfortunately, with *p* values respectively at 0.097 and 0.274, these results are not significant. Concerning the FoxM1 gene, the expression was reduced in experiment (miR-31) and control conditions (GFP) in comparison to the NT, so this is not a relevant result for the experiment condition. The low expression fold change in the GFP-treated samples may reveal a mishandling problem. Altough all these findings are statistically not significant, the reduction of the Chk1 gene expression in 661W cells, 48 hours after a miR-31 transfection is suggestive of a regulating role from miR-31 on the cell cycle. Further experiments are needed to confirm these results.

	GFP treated (control condition)	**miR-31 treated** (experiment condition)
FoxM1 fold change	0.0762	0.3458
Chk1 fold change	0.8878	0.5998
E2f4 fold change	0.9964	0.7364

Table 6: *Effects of miR-31 transfection in 661W cells on gene expressions of genes involved in cell cycle regulation. Mrl8 is the reference gene used for normalizing the data, and the genes of interest are Chk1, E2f4 and FoxM1* (n=3).

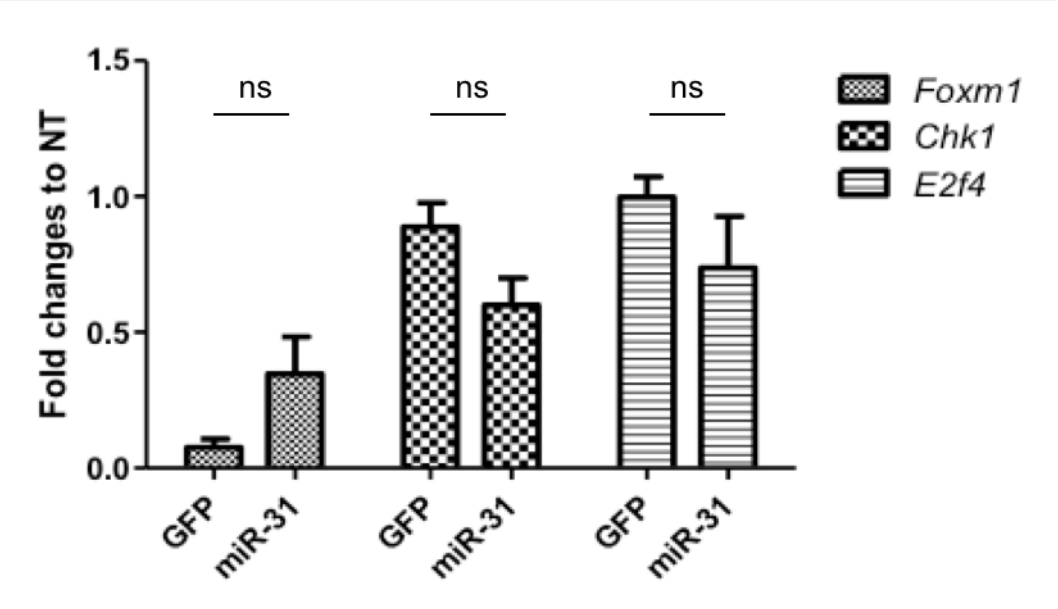

Figure 7*: Expression fold changes for Chk1, E2f4 and FoxM1 gene after miR-31 transfection in 661W cells. The results are expressed for the GFP-treated and the miR-31-treated conditions, relative to the non-treated (NT) condition. Errors bars indicate the SEM (n=3). Note that the differences are non-significant.*

Discussion

Various pathways are suspected to be involved in the retinal neurodegeneration, as PARP overactivation (16), cGMP and PKG (12) or calpain-type protease (13). Preliminary results in the laboratory showed that miR-31 concentration was reduced in degenerating *Rd1* retina, which led us to evaluate its influence on cell cycle markers. CDK2, CDK4, CDK6 and E2F1 are associated with neurodegenerative cell death (18). E2F proteins do have a major role in cell cycle progression (36) involving a huge pathway with several proteins. One of them is BMI1, which is an upstream protein of this pathway and produces a prolonged photoreceptor survival when suppressed (18). The cell cycle role in the cell death is crucial. We focused our study on CDK4 and E2F1 proteins as well as E2f4, FoxM1 and Chk1 genes. Our data highly suggests that a miR-31 overexpression is associated with a reduced E2F1 protein level. This finding does not yet lead to the full comprehension of cell death mechanism in neuronal degeneration, but it makes a potential link between E2F1 protein and miR-31 function, at least in 661W cells. And because a reduced level of E2F1 produce neuroprotective effect (18), we can suggest that miR-31 overactivation could contribute to photoreceptor survival.
In the present results FoxM1, Chk1 and E2f4 are not significantly affected by miR-31 overexpression. We may also suspect them to be indirectly targeted by miR-31, because this molecule regulates cell cycle proteins, inducing cell death (37) or inhibiting cell growth in other type of tissue (38). FoxM1 recently has been associated with other miRs as the miR-214 (39), miR-374b (40) and miR-34a (41) and they all downregulate the transcription factor. MiRs are more and more studied and their role in regulating the cell cycle is well established (28), therefore, our hypothesis seems to be realistic. With this study, we come to the suggestion that if the low concentration of miR-31 in *Rd1* retina could be increased, the amount of E2F1 protein would drop and so induce a neuroprotective effect. The link between E2F1 and miR-31 must be confirmed.
Our experiment contains limitations that are important to notice. The transfection efficiency was probably inferior to 20% for all transfection performed, despite our attempt to find the ideal transfection conditions with optimal cell culture, we think that transfection efficiency could be increased, and so improve the expression of miR-31 which may produce more considerable results. Considering this percentage of transfection, the gene expression decrease (or increase) is thus much more pronounced, because it occurred only in around 20% of the cells investigated. Moreover, all our analysis was performed on the 661W cells 48 hours after the transfection, a more extended period of time exposed to a miR-31 overexpression also could contribute to different results.
However, as this experiment was done in a short amount of time, WB analysis and qPCR could not be done for all the proteins and gene of interest, so these results can be reinforced by validating the reduction of E2F1 with qPCR. Next step could be to evaluate a miR-31 overexpression influence on other cell cycle proteins. The fact that this study was done on *in vitro* 661W cell line also has to be taken into account, as all this should be confirmed with, for example, *Rd1* retinas, and later, hopefully, with *in vivo* experiments in mice. If these results are confirmed, a test to block the cell cycle re-entry by miR-31 overexpression *in vivo* in animal models of retinal degeneration would be interesting to study a potential slowdown of the photoreceptor degeneration process.

It is worth remembering that retinal degeneration and more classic neurodegeneration in the rest of the CNS are very similar, some future findings on retinal degeneration could lead far beyond the retinitis pigmentosa and the ophthalmologic field.

Conclusion

Reduced miR-31 and reactivation of cell cycle protein in degenerating *Rd1* retina led us to the hypothesis that the degenerating process could be slowed down by blocking the cell cycle re-entry with miR-31 augmentation. The first step of the theory was confirmed by this experiment. Indeed, 48 h after a miR-31 transfection, 661W cells had a reduced E2F1 protein concentration. The possible link between E2F1 and miR-31 is important because their role in neurodegeneration may be crucial. Obviously, further studies need to legitimate our findings, but this means that miR-31 overexpresion could potentially produce a neuroprotection in degenerating cells. Next events seem to be promising as new pharmacological therapies could be developed to reduce the cell death process in degenerating retinal diseases.

Acknowledgements

I would like to thank Martial M'Befo for introducing me to the molecular biology world and for helping me in every step of the work; Prof. Yvan Arsenijevic for letting me work in his lab and for his patience; and Dana Wanner for her kind technical support.

References

1. Williamson S, Cummins H. Light and Color in Nature and Art; New York, 1983. Color Res Appl. 1985;10(2):123–4.
2. Bunker CH, Berson EL, Bromley WC, Hayes RP, Roderick TH. Prevalence of retinitis pigmentosa in Maine. Am J Ophthalmol. 1984 Mar;97(3):357–65.
3. Ayuso C, Garcia-Sandoval B, Najera C, Valverde D, Carballo M, Antiñolo G. Retinitis pigmentosa in Spain. The Spanish Multicentric and Multidisciplinary Group for Research into Retinitis Pigmentosa. Clin Genet. 1995 Sep;48(3):120–2.
4. Hartong DT, Berson EL, Dryja TP. Retinitis pigmentosa. Lancet Lond Engl. 2006 Nov 18;368(9549):1795–809.
5. Heckenlively JR, Yoser SL, Friedman LH, Oversier JJ. Clinical findings and common symptoms in retinitis pigmentosa. Am J Ophthalmol. 1988 May 15;105(5):504–11.
6. Riggs LA. The Human Electroretinogram. AMA Arch Ophthalmol. 1958 Oct 1;60(4):739–54.
7. He Y, Zhang Y, Su G. Recent advances in treatment of retinitis pigmentosa. Curr Stem Cell Res Ther. 2015;10(3):258–65.
8. Nadal J, Iglesias M. Long-term visual outcomes and rehabilitation in Usher syndrome type II after retinal implant Argus II. BMC Ophthalmol. 2018 Aug 22;18(1):205.
9. Portera-Cailliau C, Sung CH, Nathans J, Adler R. Apoptotic photoreceptor cell death in mouse models of retinitis pigmentosa. Proc Natl Acad Sci U S A. 1994 Feb 1;91(3):974–8.
10. Sahaboglu A, Paquet-Durand O, Dietter J, Dengler K, Bernhard-Kurz S, Ekström PA, et al. Retinitis pigmentosa: rapid neurodegeneration is governed by slow cell death mechanisms. Cell Death Dis. 2013 Feb 7;4:e488.
11. Pennesi ME, Michaels KV, Magee SS, Maricle A, Davin SP, Garg AK, et al. Long-term characterization of retinal degeneration in rd1 and rd10 mice using spectral domain optical coherence tomography. Invest Ophthalmol Vis Sci. 2012 Jul 10;53(8):4644–56.
12. Paquet-Durand F, Hauck SM, van Veen T, Ueffing M, Ekström P. PKG activity causes photoreceptor cell death in two retinitis pigmentosa models. J Neurochem. 2009 Feb;108(3):796–810.
13. Paquet-Durand F, Sanges D, McCall J, Silva J, Van Veen T, Marigo V, et al. Photoreceptor rescue and toxicity induced by different calpain inhibitors: Calpain in photoreceptor cell death and survival. J Neurochem. 2010 Nov;115(4):930–40.
14. Takeuchi K, Nakazawa M, Mizukoshi S. Systemic administration of nilvadipine delays photoreceptor degeneration of heterozygous retinal degeneration slow (rds) mouse. Exp Eye Res. 2008 Jan;86(1):60–9.
15. Sanz MM, Johnson LE, Ahuja S, Ekström P a. R, Romero J, van Veen T. Significant photoreceptor rescue by treatment with a combination of antioxidants in an animal model for retinal degeneration. Neuroscience. 2007 Mar 30;145(3):1120–9.
16. Paquet-Durand F, Silva J, Talukdar T, Johnson LE, Azadi S, van Veen T, et al. Excessive activation of poly(ADP-ribose) polymerase contributes to inherited photoreceptor degeneration in the retinal degeneration 1 mouse. J Neurosci Off J Soc Neurosci. 2007 Sep 19;27(38):10311–9.
17. Sancho-Pelluz J, Arango-Gonzalez B, Kustermann S, Romero FJ, van Veen T, Zrenner E, et al. Photoreceptor cell death mechanisms in inherited retinal degeneration. Mol Neurobiol. 2008 Dec;38(3):253–69.
18. Zencak D, Schouwey K, Chen D, Ekstrom P, Tanger E, Bremner R, et al. Retinal

degeneration depends on Bmi1 function and reactivation of cell cycle proteins. Proc Natl Acad Sci. 2013 Feb 12;110(7):E593–601.
19. Herrup K. Post-mitotic role of the cell cycle machinery. Curr Opin Cell Biol. 2013 Dec;25(6):711–6.
20. Gardiner KL, Downs L, Berta-Antalics AI, Santana E, Aguirre GD, Genini S. Photoreceptor proliferation and dysregulation of cell cycle genes in early onset inherited retinal degenerations. BMC Genomics. 2016 Dec;17(1).
21. Vincent I, Rosado M, Davies P. Mitotic mechanisms in Alzheimer's disease? J Cell Biol. 1996 Feb;132(3):413–25.
22. Höglinger GU, Breunig JJ, Depboylu C, Rouaux C, Michel PP, Alvarez-Fischer D, et al. The pRb/E2F cell-cycle pathway mediates cell death in Parkinson's disease. Proc Natl Acad Sci USA. 2007 Feb 27;104(9):3585–90.
23. Arsenijevic Y. Cell Cycle Proteins and Retinal Degeneration: Evidences of New Potential Therapeutic Targets. Retinal Degenerative Diseases. Springer International Publishing; 2016. p. 371–7.
24. Carrington JC, Ambros V. Role of MicroRNAs in Plant and Animal Development. Science. 2003 Jul 18;301(5631):336–8.
25. Asangani IA, Harms PW, Dodson L, Pandhi M, Kunju LP, Maher CA, et al. Genetic and epigenetic loss of microRNA-31 leads to feed-forward expression of EZH2 in melanoma. Oncotarget. 2012 Sep 1;3(9).
26. Ge F, Wang C, Wang W, Liu W, Wu B. MicroRNA-31 inhibits tumor invasion and metastasis by targeting RhoA in human gastric cancer. Oncol Rep. 2017 Jun 27;10.3892
27. Creighton CJ, Fountain MD, Yu Z, Nagaraja AK, Zhu H, Khan M, et al. Molecular profiling uncovers a p53-associated role for microRNA-31 in inhibiting the proliferation of serous ovarian carcinomas and other cancers. Cancer Res. 2010 Mar 1;70(5):1906–15.
28. Bueno MJ, Malumbres M. MicroRNAs and the cell cycle. Biochim Biophys Acta BBA - Mol Basis Dis. 2011 May 1;1812(5):592–601.
29. Mastropasqua R, Toto L, Cipollone F, Santovito D, Carpineto P, Mastropasqua L. Role of microRNAs in the modulation of diabetic retinopathy. Prog Retin Eye Res. 2014 Nov;43:92–107.
30. Suárez Y, Fernández-Hernando C, Yu J, Gerber SA, Harrison KD, Pober JS, et al. Dicer-dependent endothelial microRNAs are necessary for postnatal angiogenesis. Proc Natl Acad Sci USA. 2008 Sep 16;105(37):14082–7.
31. Kurihara H, Maruyama R, Ishiguro K, Kanno S, Yamamoto I, Ishigami K, et al. The relationship between EZH2 expression and microRNA-31 in colorectal cancer and the role in evolution of the serrated pathway. Oncotarget. 2016 Mar 15;7(11):12704–17.
32. Shen J, Yang X, Xie B, Chen Y, Swaim M, Hackett SF, et al. MicroRNAs Regulate Ocular Neovascularization. Mol Ther. 2008 Jul;16(7):1208–16.
33. Yu T, Ma P, Wu D, Shu Y, Gao W. Functions and mechanisms of microRNA-31 in human cancers. Biomed Pharmacother. 2018 Dec 1;108:1162–9.
34. Li T, Luo W, Liu K, Lv X, Xi T. miR-31 promotes proliferation of colon cancer cells by targeting E2F2. Biotechnol Lett. 2015 Mar;37(3):523–32.
35. Sayyad Z, Sirohi K, Radha V, Swarup G. 661W is a retinal ganglion precursor-like cell line in which glaucoma-associated optineurin mutants induce cell death selectively. Sci Rep. 2017 Dec 4;7(1):16855.
36. Ren B, Cam H, Takahashi Y, Volkert T, Terragni J, Young RA, et al. E2F integrates cell cycle progression with DNA repair, replication, and G2/M checkpoints. Genes Dev. 2002 Jan

15;16(2):245–56.
37. Zhang J, Xu D, Li N, Li Y, He Y, Hu X, et al. Downregulation of microRNA-31 inhibits proliferation and induces apoptosis by targeting HIF1AN in human keloid. Oncotarget. 2017 Sep 26;8(43):74623–34.
38. Kim HS, Lee KS, Bae HJ, Eun JW, Shen Q, Park SJ, et al. MicroRNA-31 functions as a tumor suppressor by regulating cell cycle and epithelial-mesenchymal transition regulatory proteins in liver cancer. Oncotarget. 2015 Mar 10;6(10):8089–102.
39. Tian C, Wu H, Li C, Tian X, Sun Y, Liu E, et al. Downreguation of FoxM1 by miR-214 inhibits proliferation and migration in hepatocellular carcinoma. Gene Ther. 2018;25(4):312–9.
40. Xia N, Tan W-F, Peng Q-Z, Cai H-N. MiR-374b reduces cell proliferation and cell invasion of cervical cancer through regulating FOXM1. Eur Rev Med Pharmacol Sci. 2019 Jan;23(2):513–21.
41. Zhou H, Yang L, Xu X, Lu M, Guo R, Li D, et al. miR-34a inhibits esophageal squamous cell carcinoma progression via regulation of FOXM1. Oncol Lett. 2019 Jan;17(1):706–12.